Preparation and characterization of Li₂O-CaO-Al₂O₃-P₂O₅-SiO₂ glasses as bioactive material

3.1. Introduction:

Bioactive glasses have been widely investigated for bone repair because of their outstanding bioactive properties. However, bioactive materials undergo incomplete conversion into a bone like material which limits their biomedical application (Hench, 1991). In simulated body fluid, bioactive glasses bind to living bone through an apatite layer formed on their surfaces (Bohner *et al*., 2009). The bonding mechanism of implant to the bone was given by Clark and Hench (Clark *et al*., 1976). Hench decided to make a glass of the SiO_2-Na_2O-CaO-P_2O_5 system containing high calcium contents with a composition close to a ternary eutectic in the Na_2O–CaO–SiO_2 diagram (Hench, 2006). The main discovery was that a glass of the mol% composition $46.1SiO_2$-$24.4Na_2O$-$26.9CaO$-$2.6 P_2O_5$, known as 45S5 bioglass, formed a strong bond with bone which could not be removed without breaking the bone (Hench *et al*., 1971). This launched the field of bioactive ceramics with many new materials and products (Hench, 2006, Kokubo, 1991 and LeGeros, 2002). 45S5 is widely used in biomedical devices such as middle ear and dental implants. However, relatively low strength and brittleness limits its application to non-load-bearing situations (Cao *et al*., 1996). Interest has also increased in borate glasses mainly due to very encouraging clinical results of healing the harmful chronic wounds like diabetic and ulcers (Rahaman *et al*., 2011 and Jung *et al*., 2011). The benefits of phosphate glasses are related to their very rapid solubility like borate glasses rather than bioactivity (Abou *et al*., 2009).

The 45S5 glass tends to crystallize at high temperature like other bioactive glasses due to its relatively low silica content (Arstila *et al*., 2008). It was a relevant drawback because the crystallization had reduced the bioactivity of the glass (Shirtliff *et al*., 2003 and Li *et al*., 1992). The addition of elements like magnesium, aluminum, zirconia or titanium may be used to control some physical and chemical properties of bioglasses (Agathopoulos *et al*., 2006 and Marti, 2000). Many systematic investigations have been carried out by earlier workers to check the effect of alumina on bioactivity and mechanical properties of phosphate, silicate and phosphor silicate based bioglasses and bioglass-ceramics, but the role of Al_2O_3 for Li_2O has never been investigated in such systems (El-Kheshen *et al*., 2008). The addition of Al_2O_3 to the bioactive glass is expected to improve the repair in bone defect and to control the degradation rate for long-term stability of the implants. Sitarz *et al*. (Sitarz *et al*., 2010) has observed that addition of Al^{3+} in proper concentration increased the mechanical resistance of the bioglasses. The presence of Al_2O_3 results in the breaking of P=O bonds and the Si–O–P linkages are replaced by Al–O–P linkages in the glass network which prevents the degradation (Sitarz, 2010). However, Al_2O_3 addition in higher concentrations to the borate free silicate-based bioactive glass is not desirable due to the ability to damage the genome or to disrupt the cellular metabolic processes and harmful impact on the bioactivity of glass (Ohtsuki *et al*., 1992 and Gross *et al*., 1985). In recent years, the earlier work has shown the increasing effect of lithium on bone density. The anabolic effect of lithium on the mass density of bone in mice had shown by Clement *et al*. (Clement *et al*., 2005). The maintenance therapy with lithium can safely preserve and intensify bone density as earlier reported by Zamani *et al*. (Zamani *et al*., 2009). Although the role of Al_2O_3 in glass is commonly different from

that of Li_2O but the molar addition of 0.5 to 2.5 mol% Al_2O_3 for Li_2O in glass was done on the basis of the earlier concepts in order to improve the required properties of the glass. The purpose of substitution of Al_2O_3 for Li_2O is to improve the structural properties and the bioactivity of the glass and prepare a bioactive glass which can be mechanically as well as hydrolytically stable as an implant material.

The aim of this work in other words is to provide information on assessment of bioactivity through *in vitro* test in SBF and to increase the physio-chemical as well as mechanical properties of base bioactive glass by introducing 0.5 to 2.5 mol% Al_2O_3 into it. Therefore, in the present investigation, the concentration of Li_2O was varied by mol% addition of Al_2O_3 from 0.5 to 2.5.

3.2. Experimental Procedure

3.2.1 Materials and methods

The mol% compositions and ratio of Al_2O_3 to Li_2O of the bioglass samples have been given in table 3.1. Fine-grained quartz was used as a source of SiO_2. Analytical reagent grades $CaCO_3$, Li_2CO_3 and $(NH_4)H_2PO_4$ were used as a source of CaO, Li_2O and P_2O_5, respectively. The required amounts of analytical reagent grade Al_2O_3 were added in the batch for the partial substitution of Li_2O. The raw materials for different samples were properly weighed. Then the mixing of different batches was done for 30 min and after that, they were melted in a 100 ml platinum–2% rhodium crucible at 1400°C in the air as furnace atmosphere. The temperature of the furnace was controlled within ±10°C by an automatic temperature indicator-cum controller. The thermal cycle was set for the all glass samples from room temperature to 1000°C at the 10°C min^{-1}. Further, it was held at 1000°C for 1 h and heated from 1000 to 1400°C at the rate of 10°C min^{-1} and again held

at 1400°C for 2 h. The melting of samples was done in the electric globar furnace in air as the furnace atmosphere. The melted samples were poured on a preheated aluminium sheet and directly transferred to a regulated muffle furnace at 450°C for annealing.

After 1 h of annealing of the samples, the furnace was cooled to the room temperature at the controlled rate of cooling. The samples were crushed in a pestle mortar and then ground in an agate mortar to make fine powders of the samples for different properties measurements by different experimental techniques.

Table 3.1. Mol% composition of the bioactive glass samples.

Sl. No.	SAMPLES	SiO_2	CaO	P_2O_5	Li_2O	Al_2O_3	Al_2O_3 / Li_2O ratio
1.	LiAl0.0	42	34	6	18	0	0.00
2.	LiAl0.5	42	34	6	17.5	0.5	0.028
3.	LiAl1.0	42	34	6	17	1.0	0.058
4.	LiAl1.5	42	34	6	16.5	1.5	0.090
5.	LiAl2.5	42	34	6	15.5	2.5	0.161

A part of the annealed bioactive glass samples was cut, ground and polished for measurement of its physical and mechanical properties. The *in vitro* bioactivity of these samples was assessed by immersion in SBF solution for different time periods under physiological conditions. The formation of hydroxy carbonate apatite (HCA) layer on the surface of the glass samples after SBF treatment was confirmed by FTIR, XRD and SEM as well as pH measurement.

3.2.2 *In vitro* biocompatibility study

The *in vitro* cell viability and cytotoxicity of bioactive glass samples against osteoblast (MG63) cell lines have been performed in order to assess the biocompatibility. The human osteoblast MG63 cell lines (ATCC, USA) were used in this investigation. The bioactive glass samples were sterilized in an autoclave at 121°C for 30 min. MG63 cells were cultured in a minimum essential medium (MEM; Invitrogen Corporation), augmented with 10% of foetal calf serum (FCS), 1% antibiotic antimycotic solution in a humidified atmosphere at 37°C and with 5% CO_2 for 24, 48 and 72 h. The methyl thiazolyl tetrazolium (MTT) [3-(4, 5-dimethylthiazol-2-yl)-2, 5-diphenyl tetrazolium bromide] assay was used for evaluating the cell viability (Kapusetti *et al*., 2014) and cytotoxicity (Kapusetti *et al*., 2012).

3. Results and discussion

3.1 Mechanical properties

3.1.1 Density and compressive strength

Fig. 3.1 and 3.2 shows the density and compressive strength of the glass samples as a function of Al_2O_3/ Li_2O ratio. From Fig. 3.1 it is clear that an increase in Al_2O_3 substitution up to 1.0 mol% resulted in an increase in the density of glass samples from 2.68 to 2.77 gm/cc but further beyond that up to 2.5 mol% it tends to saturate at 2.83 gm/cc in the glass. This is attributed due to the reason that lighter element lithium has been replaced by heavier element aluminum up to a limited substitution of 1.0 mol% Al_2O_3. However, the tendency towards saturation of density beyond 1.0 mol% Al_2O_3 can be due to compensating free volume increase with increasing aluminium leading to asymptotic behavior of density changes in the glass samples.
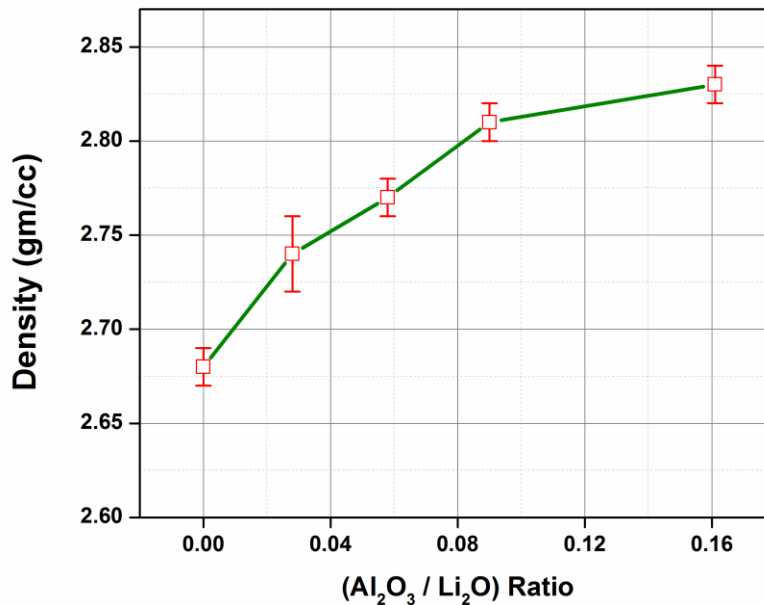
Fig. 3.1: Variation in density with Al_2O_3/Li_2O ratio in bioglass samples LiAl0.0 to LiAl2.5.

On the other hand, the compressive strength of the glass system has also been found to increase with increasing Al_2O_3/ Li_2O ratio in the glass (Fig. 3.2) as the bigger Li+ ion (0.59 Å) has been replaced by a smaller Al^{3+} ion (0.39 Å) in tetrahedral co-ordination (Shannon, 1976) in the glass system. It was expected that the low expansion produced by smaller Al^{3+} ion had resulted a high surface compression giving high strength in the bioactive glass samples. Chemical strengthening of glass by ion exchange process is done not only by replacement of a smaller ion by a bigger ion but also vice-versa with an exchange of a bigger ion by a smaller ion in the glass (Scholes, 1975). Although the role of Al_2O_3 as an intermediate oxide in the glass structure has been reported to be different from that of alkali oxides as modifiers but substitution of Li_2O for Al_2O_3 in glass has

been reported by earlier workers (Andersson *et al*., 1999, Branda *et al*., 2001 and Mirhadia *et al*., 2012).
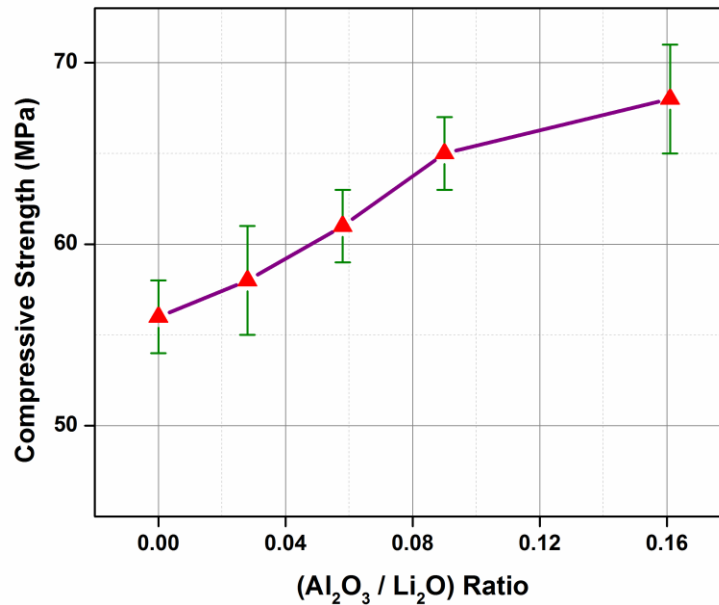

Fig. 3.2: Variation in compressive strength with Al_2O_3/Li_2O ratio in bioglass samples (LiAl0.0 to LiAl2.5).

3.1.2 Elastic modulus, shear modulus and bulk modulus

Fig. 3.3 shows an increase in the elastic modulus, shear modulus and bulk modulus with increasing Al_2O_3/Li_2O ratio in the glass samples. The Fig. 3.3 also represents the experimental values of the elastic moduli, Young's modulus (E), shear modulus (S), bulk modulus (K) of the bioglasses. All the elastic moduli values were found to increase with increasing Al_2O_3/Li_2O ratio. The elastic moduli of the bioglass samples show similar trends regarding improvement in their mechanical properties with the variations in the ultrasonic velocities.
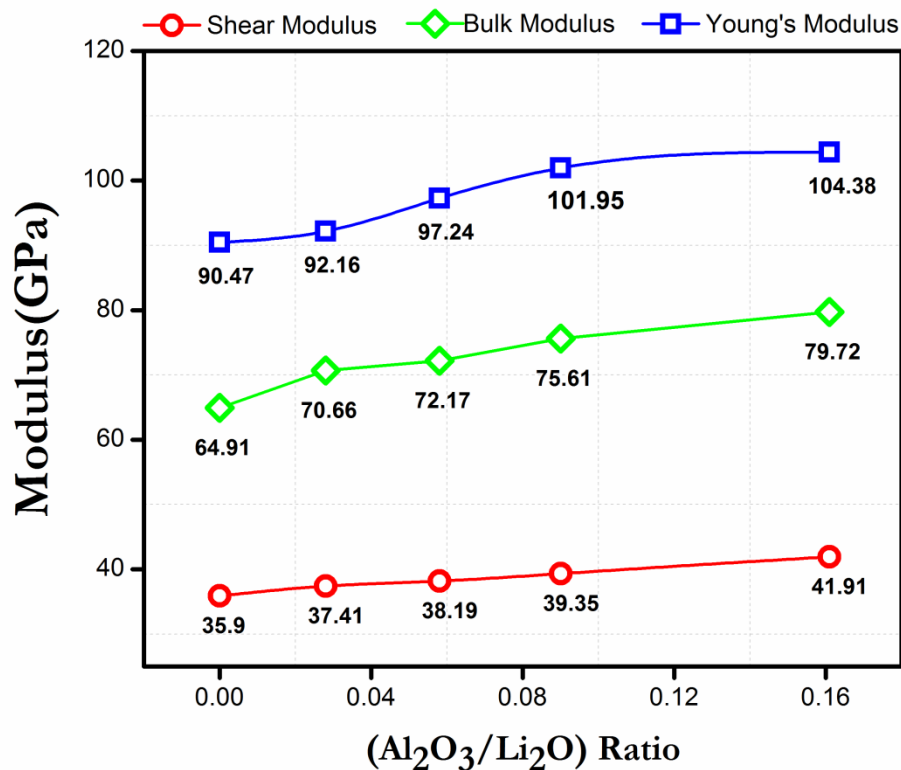
Fig. 3.3: Elastic modulus, shear modulus and bulk modulus of all bioglass samples (LiAl0.0-LiAl2.5).

Young's modulus dictates the stiffness of materials, which is also attributed to the greater bond strength between the atoms in a material. Hence, higher the Young's modulus, greater the stiffness of the material and closer would be the bonding (Vallet *et al.*, 2005). As shown in Fig. 3.3 that an increase in Young's modulus, Shear modulus and Bulk modulus of the bioglass samples is due to increase in bridging oxygens (-O-) by addition of Al_2O_3 in the glass structure which is also evident from the FTIR absorption bands observed at 432 and 745 cm^{-1} for AlO_6 and AlO_4 units (Fig 3.10 (a)). On increasing the concentration of Al_2O_3 beyond 1.5 mol%, AlO_4 units prevail in the glass matrix which results in an increase in the number of bridging oxygens. Thus bridging oxygens (-O-) have improved the connectivity of the glass network. Earlier, it has been also shown that

addition of Al_2O_3 for Na_2O in a sodium silicate glass has increased the Young's modulus of the glass (Paul, 1990). Thus, the structure of glass becomes more rigid and stiff which resulted in an increase in Young's modulus from 90.47 to 104.38 GPa with increasing Al_2O_3 content in the base bioglass. Further, an increase in shear modulus (35.90 to 41.91 GPa) and bulk modulus (64.91 to 79.72 GPa) has also confirmed the improvement in elastic properties of the glass samples.

3.1.3 Vickers hardness

It can be seen from Fig. 3.4 that the Vickers hardness of the bioglass samples has increased gradually as $Al_2O_3/$ Li_2O ratio increased. The mean values of Vickers hardness of samples have been taken with several trials and presented in the form of error bars. Since the binding energy (Columbic force $= ZZ'/(r +r0)^2$ where Z and Z´ are the charge on the cations and O^{2-} ion; r and r0 are ionic radii of cations and O^{2-} ion, respectively) between Al^{3+} and O^{2-} ions have increased comparatively more than Li^+ and O^{2-} ions in the glass resulting in bond strengthening with Al_2O_3 addition. It is mentioned herewith that the replacement of bigger Li^+ by smaller Al^{3+} ion has not only increased the bond strength by increasing the multiple of charge (ZZ´) but the same has also resulted in strengthening due to smaller ionic radii of Al^{3+} than Li^+ ion. This would naturally compress the structure and thus improving the hardness of the glass samples (Varshneya, 2006). So replacement of lithia by alumina on molar basis had enhanced the mechanical properties of the bioglass samples as also evident from the results presented in the Figs. (3.1-3.4). Therefore, it increased the densities and resulted in creating new bonds with incorporation of aluminium ions. It has caused reinforcement of the glass structure and

resulted in improvement in the compression of the glass and thus preventing the penetration in the glass system.
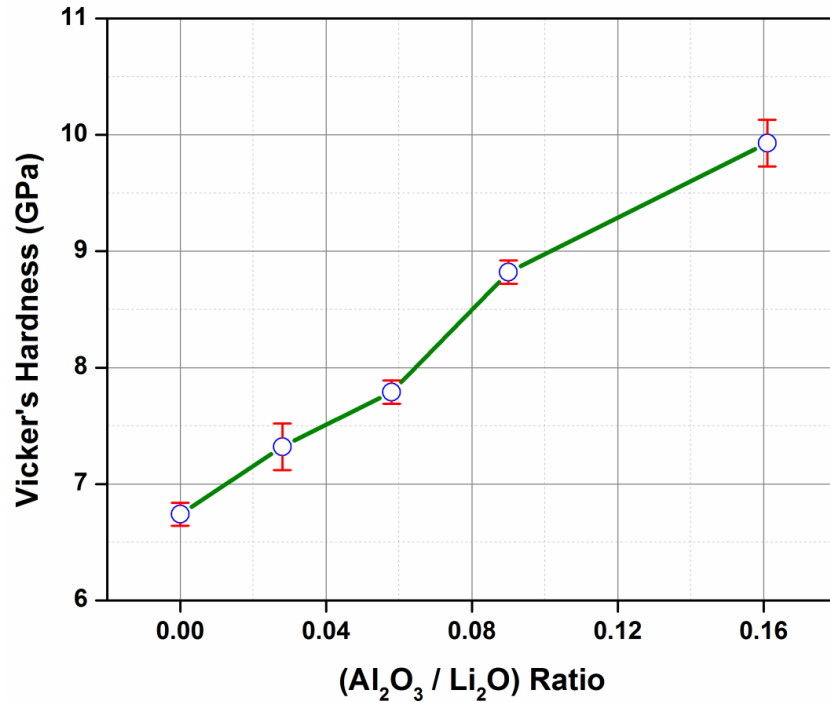

Fig. 3.4: Vickers hardness of the bioglass samples (LiAl0.0-LiAl2.5).

Same time the alumina is well known to prevent the devitrification of glass and also it increases tremendously the chemical durability of glasses (Paul *et al.*, 1978 and Teixeira *et al.*, 2007). That is why the Vickers hardness of the bioglass samples had increased with increasing amount of Al_2O_3 in glass.

El-Kheshen *et al.* (El-Kheshen *et al.*, 2008) have also investigated the effect of Al_2O_3 addition on bioactivity and mechanical properties of soda-lime-alumino-phosphate bioactive glasses and found that Al_2O_3 has appreciably increased the hardness of the glass. Sitarz *et al.* (Sitarz *et al.*, 2010) have also studied influence of alumina on the structure and texture of alkali-alkaline earth-phospho-silicate and alkali-alkaline earth-alumino-phospho-silicate glasses and spectroscopically established its homogenizing

effect on structure of glass. The authors have mentioned that addition of small amount of alumina (5 mol% of $AlPO_4$) has caused a change in composition of the glassy matrix and inclusions and thereby making it mechanically more stable. The observations made by earlier workers (El-Kheshen *et al*., 2008, Sitarz *et al*., 2010 and Sitarz, 2010) support our present results regarding improvement of mechanical properties of bioglasses by substitution of alumina at the cost of lithia.

3.2 pH behavior of the samples in SBF solution

Fig. 3.5 shows the variation of pH of bioactive glass samples after immersing in simulated body fluid (SBF) solution up to 28 days. It shows that for all bioactive glass samples, the pH increases within 1 to 3 days as compared to the initial pH of the SBF solution at 7.4 under physiological condition. The increase in pH values is due to fast release of cations through exchange with H^+ or H_3O^+ ions in the simulated body fluid (SBF) solution. The H^+ ions are being replaced by cations which cause an increase in hydroxyl concentration of the solution (Filguei ras *et al*., 1993). This leads to attack on the silica glass network, which results silanols formation leading to decrease in pH after 3 days as indicated in the Fig. 3.5 when bioactive glass samples were immersed in simulated body fluid (SBF) solution up to 28 days. The change in pH was due to leaching of cations. The increase in pH of SBF solution shows a decrease in the concentration of H^+ ions due to the replacement of cations in the bioactive glasses. The Fig. 3.5 shows that addition of alumina up to 1.5 mol% resulted in an increase in pH of the SBF solution containing immersed samples which attained maxima after around three days and then it

decreased with time referring to base glass sample. The high degradation rate leads to higher pH value. So, an
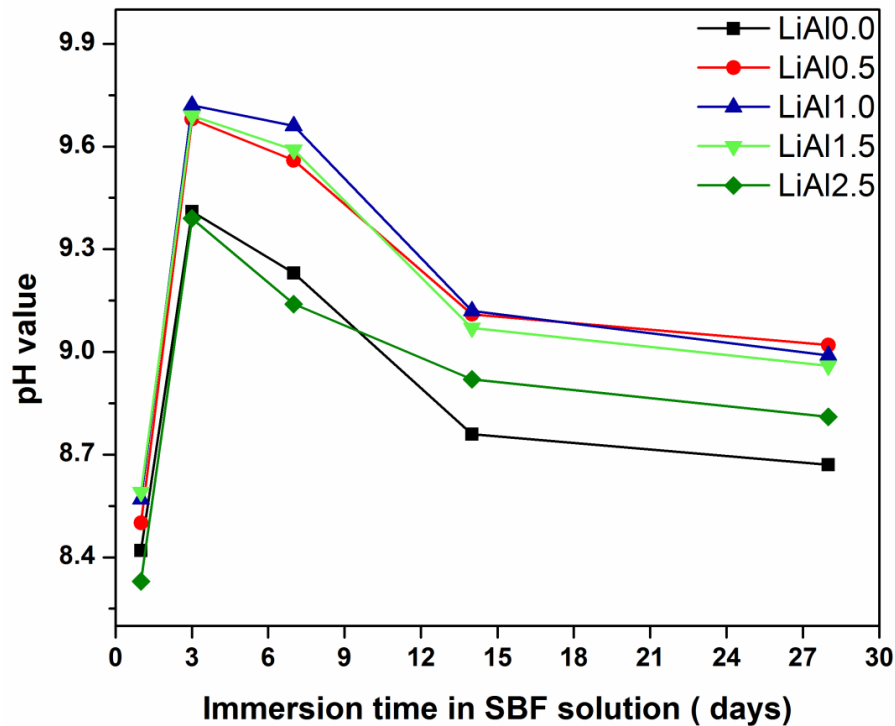

Fig. 3.5: Variation of pH of bioactive glass samples (LiAl0.0 to LiAl2.5) after immersing in simulated body fluid (SBF) up to 28 days.

increase in the pH value of SBF solution also favors the hydroxy carbonate apatite formation. However, the addition of Al_2O_3 beyond 1.5 mol% caused a decrease in maxima of the pH of SBF solution containing immersed sample. This dictates that addition of Al_2O_3 up to 1.5 mol% in the glass samples has increased its bioactivity, but beyond 1.5 mol% of Al_2O_3 retards the bioactivity of the glass samples (Fig. 3.5). This observation can be explained in the manner that addition of Al_2O_3 up to 1.5 mol% goes into formation of AlO_6 octahedra and produces more of non-bridging oxygens which results in an increase in bioactivity of samples. Whereas further addition of Al_2O_3 beyond 1.5 mol% results in the formation of AlO_4 tetrahedra which causes a decrease in the

bioactivity of the samples. However, previous investigations made by Belkebir *et al.* (Belkebir *et al.* 1999) had pointed out that AlO_6 octahedra dominated the glass structure when Al_2O_3 was present in small concentrations, but AlO_4 tetrahedral units prevailed when Al_2O_3 concentration was higher. MAS-NMR studies made earlier in glasses with 27Al by Muller *et al.* (Muller *et al.*, 1983) and Brow *et al.* (Brow *et al.*, 1997) have revealed that aluminium ions occupy both tetrahedral sites with AlO_4 network former and octahedral with AlO_6 network modifier in the structure according to their suggested mechanism. So, the AlO_4 tetrahedra increases the strength of the glass and on the other hand AlO_6 octahedra increases the bioactivity of the bioglass samples. Greenspan *et al.* (Greenspan *et al.*, 1976) also confirmed that the change in pH of glass samples took place after immersion in simulated body fluid (SBF) solution. Morphological properties of bioactive glasses also indicate that soaking in SBF solution leads to formation of hydroxy apatite layer on the surface of the samples (Hayakawa *et al.*, 1999 and Kasuga *et al.*, 2001). The maxima of pH values were recorded on the third days as pH= 9.41, 9.68, 9.72, 9.69 and 9.39 for the samples LiAl0.0 to LiAl2.5 respectively at 37°C under physiological condition, which is due to the fast dissolution rate. The addition of Al_2O_3 up to 1.5 mol% the maxima of pH is more than the base glass, but beyond that it is lower than the base glass sample. This may influence formation of the apatite layer on the surface of the glass samples at an early stage (Filgueitras *et al.*, 1993). The earlier investigations done by Majhi *et al.* (Majhi *et al.*, 2012) regarding the pH behavior of SBF solution containing immersed bioglass and bioglass ceramic samples has also confirmed formation of hydroxy carbonate apatite layer on the surface of the samples showing its bioactivity. In the initial stages the authors found that the pH of the solution increased

with increasing immersion time which attained maxima and then it decreased continuously with increasing time. This confirms that the bioactivity of a particular sample attains maxima only after a specific period of time which shows its maximum bioactivity at this point of time. The maxima in bioactivity were found to vary from one sample to another depending upon the bioglass and bioglass ceramic compositions (Majhi *et al*., 2011, 2011). When bone is formed, the cross linking of the collagen chains and the subsequent precipitation of hydroxyl carbonate apatite is pH dependent and require a high pH at the bone formation site (Groot *et al*., 1998). Ohtsuki and Kokubo (Ohtsuki *et al*., 1992) had earlier investigated the effect of Al_2O_3 on bioactivity of $CaO\text{-}SiO_2\text{-}Al_2O_3$ glasses by *in vitro* tests. They evaluated the bioactivity of the glass samples by hydroxy apatite formation on the surface of these glasses using various instrumental techniques and found that calcium alumino silicate containing less than 1.5 mol% Al_2O_3 formed the apatite layer on the surface of the glass, but glasses containing more than 1.7 mol% of Al_2O_3 did not form this layer. The authors (Ohtsuki *et al*., 1992) have mentioned with well known fact that glasses and glass ceramics form interfacial bonds with living bone due to formation of an apatite layer on the surface of these systems. The apatite layer on the surface can be reproduced even in acellular SBF which has almost equal concentrations of ions to those of human blood plasma. Moreover, Bohmer and Lematre (Bohner *et al*., 2009) after critical review had also mentioned the *in vitro* method for testing the extent of bone bonding of a biomaterial and they said that it was a very attractive concept. The results of the present investigations entirely based on the well established *in vitro* tests are well supported by earlier studies (Ohtsuki *et al*., 1992, Majhi *et al*., 2011).

3.3 *In vitro* bioactivity of bioglasses by X-ray difractometry

X-ray diffraction patterns were observed using a Rigaku portable XRD machine (Rigaku, Tokyo, Japan). Phase identification analysis was carried out by comparing the XRD patterns of the bioactive glass samples to the standard database stated by JCPDF. Fig. 3.6 shows the XRD patterns of the bioactive glass samples before soaking them into the simulated body fluid (SBF). Before being soaked in SBF solutions, there was no XRD absorption peak for the bioactive glass samples, except a bump like peak ranging from 20° to 30°, which is due to Si-O-Si network. So,
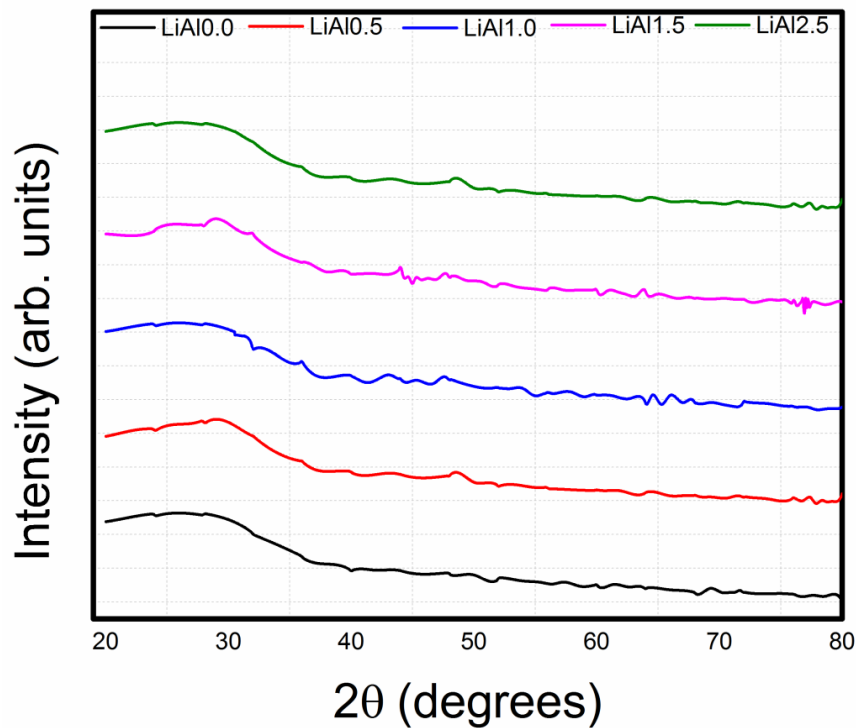

Fig. 3.6: XRD patterns of the bioactive glass samples (LiAl0.0 to LiAl2.5) before soaking them into the simulated body fluid solution.

it is clear that bioactive glass samples were amorphous in nature before being soaked in simulated body fluid (SBF) solution. Fig. 3.7 shows the XRD patterns of the bioactive glass samples soaked in the simulated body fluid (SBF) solution for 14 days. After being

soaked in the SBF solution for 14 days, one broad diffraction peak was observed at 30-32° of 2θ angle, corresponding to the HA phase (Groot *et al.*, 1998). These peaks were identified by standard JCPDS cards numbered 89-6495. In fact, the XRD patterns of bioglass samples which have broad ''humps'' centered around 2θ =31°, confirm the amorphous nature of the hydroxy carbonate apatite (Brovarone *et al.*, 2006).
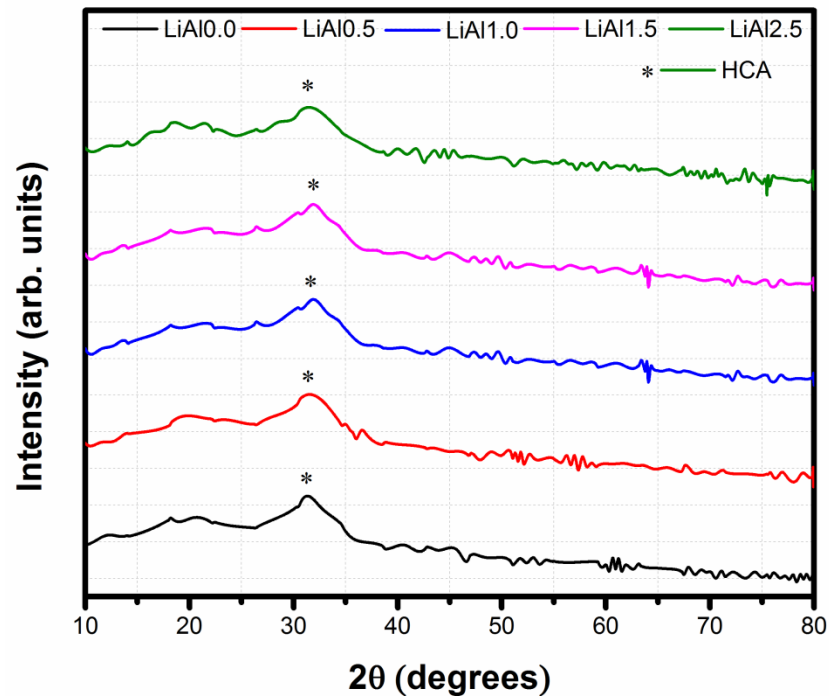

Fig. 3.7: XRD patterns of the bioactive glass samples (LiAl0.0 to LiAl2.5) soaked in the simulated body fluid solution for 14 days.

3.4 SEM analysis of bioactive glass samples

The SEM micrographs of bioactive glass samples before soaking in SBF solution are shown in Fig. 3.8 (a, b, c, d and e) which shows different rod type structure and irregular grain of bioactive glass samples which are quite similar to the result found by Hanan *et al.* (Hanan *et al.*, 2009).
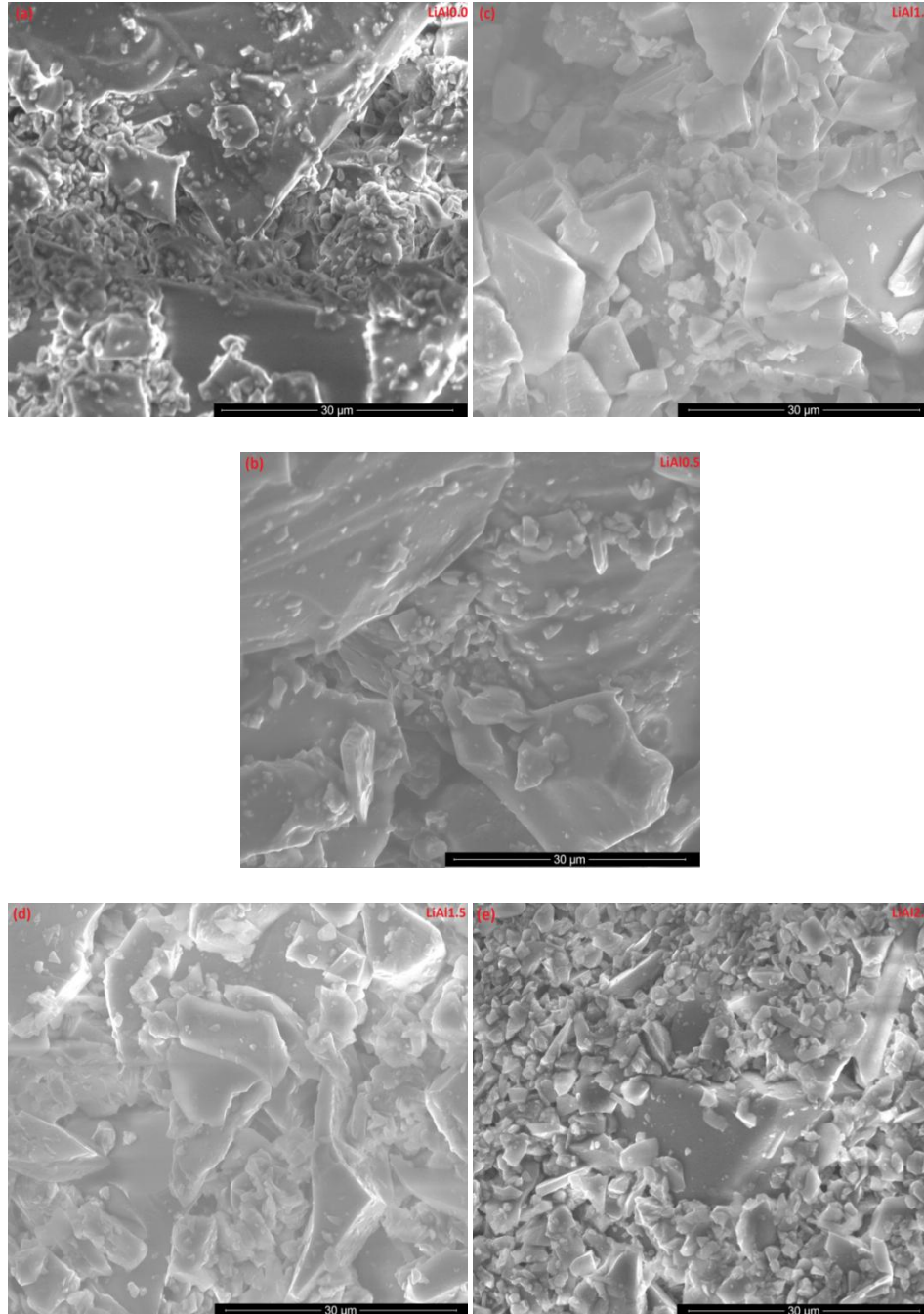
Fig. 3.8 (a–e): SEM micrographs of bioactive glass samples (LiAl0.0 to LiAl2.5) before soaking in SBF solution.

Fig. 3.9 (a, b, c, d and e) shows the SEM micrographs of bioactive glass samples after soaking in SBF solution for 28 days. It is clear from the Fig. 3.9 that bioactive glass samples which were soaked in SBF solution for 28 days were covered with irregular

shape and grounded HA particles have been grown into several agglomerates consisting of HA layer. These micrographs show the formation of HA on the surface of bioactive glass samples after immersion in SBF solution for 28 days.
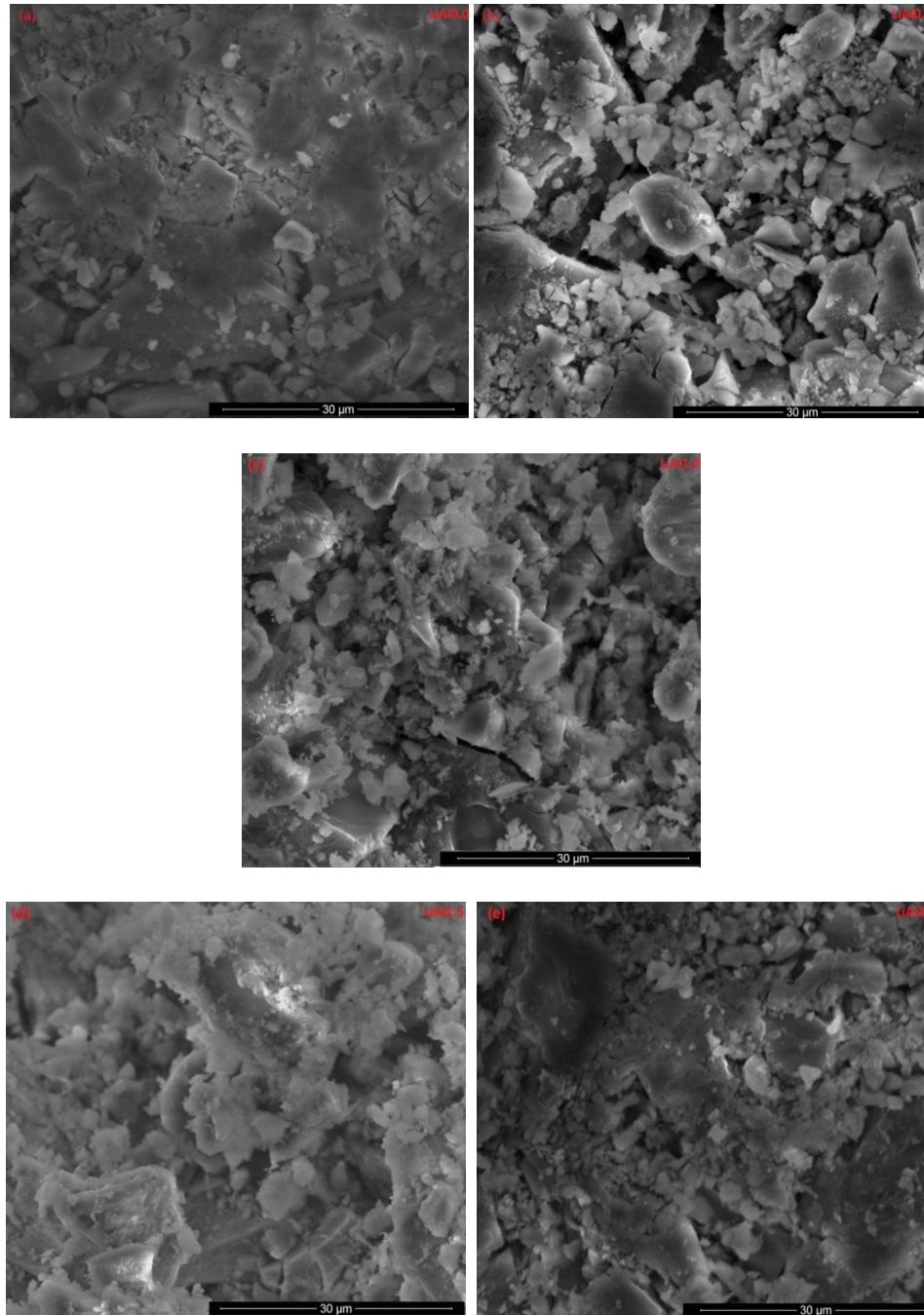

Fig. 3.9 (a–e): SEM micrographs of bioactive glass samples (LiAl0.0 to LiAl2.5) which were soaked in SBF solution for 28 days.

3.5 FTIR-Spectrometry

Fig. 3.10 (a-d) shows the FTIR absorption spectra of various bioglass samples for a plot of log (1/R) versus wavenumber before and after soaking them into SBF solution for different time intervals. Fig 3.10 (a) shows the absorption spectra of all bioglass samples before soaking them in SBF solution. The FTIR spectra of glass samples before immersion in SBF solution exhibit vibrational bands at around 432 cm^{-1} due to Si-O-Si bending/AlO$_6$ units & 635 cm^{-1} due to Si-O-Si bending (Nakamura *et al.*, 1984 and Kusabiraki, 1986), , 870, 970 & 1200 cm^{-1} due to Si-O-Si asymmetric stretching (Goh *et al.*, 2014 and Cerruti *et al.*, 2005), 748 cm^{-1} due to AlO$_4$ units (Mohini *et al.*, 2013) and 1990 cm^{-1} due to O-H stretching mode of vibrations. Fig 3.10 (b) shows the absorption spectra of all bioglass samples after soaking into SBF solution for 1 day. The new bands were observed at 1638 & 3390 cm^{-1} in the spectra which are attributed due to presence of OH group because of water adsorption in the system (Stoch *et al.*, 1999).

Fig 3.10(c) shows the absorption spectra of all bioglass samples after soaking into SBF solution for 3 days. The spectra reveal that after soaking the samples for duration of 3 days, some additional peak was found in the spectra of bioglass samples centered at 546 cm^{-1} due to calcium phosphate (hydroxyapatite) surface layer which indicate the formation of apatite in SBF solution (ElBatal *et al.*, 2003). In addition to these other bands were also found to be centered at around 1420 and 1480 cm^{-1} which are attributed due to carbonate groups (CO$_3$)$^{2-}$ indicating the precipitation of B-type hydroxy carbonate apatite, (Ca$_9$(HPO$_4$)$_{0:5}$ (CO$_3$)$_{0:5}$(PO$_4$)$_5$OH) (HCA) mimicking bone like apatite in the system (Macon *et al.*, 2015). Fig 3.10 (d) shows the absorption spectra of all bioglass samples after soaking into SBF solution for 7 days. It is evident from the spectra that

some additional bands at around 960 cm^{-1} due to P-O stretching in apatite like structures (Macon *et al*., 2015) as well as 1420 and 1480 cm^{-1} due to carbonate groups $(CO3)^{2-}$ (Kutbay *et al*., 2014) have appeared in the system as a result of SBF treatment for a period of 7 days.
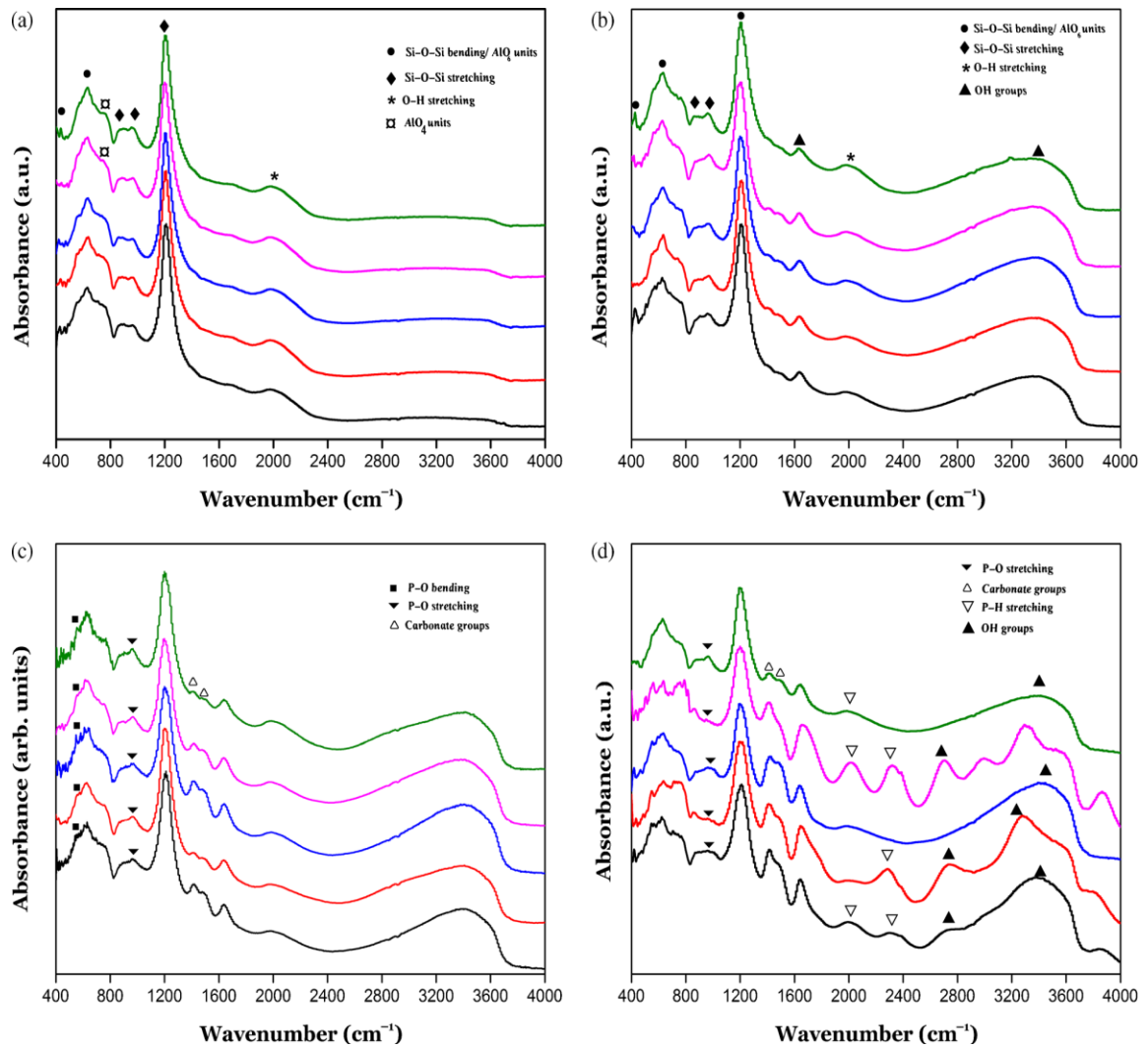

Fig. 3.10: FTIR absorption spectra of all glass samples (a) before soaking them into SBF solution, (b) after soaking them into SBF for 1 day, (c) after soaking them into SBF for 3 day and (d) after soaking them into SBF for 7 days.

The absorption bands around 2010 and 2300 cm^{-1} were attributed due to P-H stretching modes as well as 2743 and 3400 cm^{-1} is due to O-H stretching mode of vibrations (Macon

et al., 2015). The formation of hydroxy carbonate apatite (HCA) layer takes place after the immersion of the samples in the SBF solution and the mechanism for the formation of HCA layer on the surface of the samples has been earlier explained by Hench in bioactive glasses (Hench, 1991) which bond the implant to the body bones and other tissues. The mechanism of hydroxyapatite formation followed by cation exchange involves the formation of silica-rich layer at the surface of the glass which contains Si–OH groups that act as nucleation sites for amorphous calcium–phosphate (Kutbay *et al*., 2014). The increase in pH promotes crystallization of calcium–phosphate (Ca-P) where the tetrahedral $(PO_4)^{3-}$ exhibits sharp IR absorptions at 546 cm^{-1} characteristic to P-O bending. The absorption spectra of bioactive glass samples showed the P-O bending vibrational bands after 3 days of immersion in SBF. Other bands marked at 1420 and 1480 cm^{-1} were characteristic of carbonate group, $(CO_3)^{2-}$ indicating the precipitation of B-type hydroxy carbonate apatite (HCA), $Ca_9(HPO_4)_{0.5}(CO_3)_{0.5}(PO_4)_5OH$. The precipitation of pure hydroxyapatite in SBF is likely to happen less because it is saturated with respect to slightly carbonated apatite, in which the orthophosphates are substituted with carbonates in the crystal lattice (Elliot, 1994). Gibson *et al* (Gibson *et al*., 2000) pointed out that the P–O bending bands, at 546 cm^{-1} in the FTIR spectra were not characteristic to HA or HCA, but they do indicate the presence of orthophosphate lattices. Therefore, the newly phase formed at the surface of the bioactive glass samples were also confirmed by X-ray diffraction as shown in Fig. 3.7. So our results regarding formation of HCA in SBF by FTIR absorption spectrometry are well supported by the observations made by Macon *et al* (Macon *et al*., 2015).

3.6 *In vitro* **biocompatibility study**

The viability and cytotoxicity of bioactive glass samples was assessed using MG63 cell lines and the percent viability and cytotoxicity of the samples was measured with respect to time. The number of living cells proliferated was determined by MTT assay on the sample's surface. The optical density of the solution was measured to quantify the cell viability/living cell count. The cell viability and cytotoxicity for bioactive glass samples have been plotted as a function of time and presented in Figs. 3.11 and 3.12, respectively. The Figs. 3.11 & 3.12 clearly show a decreasing trend in cell viability and increasing in cytotoxicity with an increase in Al_2O_3 concentration beyond 1.0 mol%. Fig. 3.11 dictates the cell viability against MG63 cell lines and the results show that the cell viability was greater than 80% even after 72 h of culture.
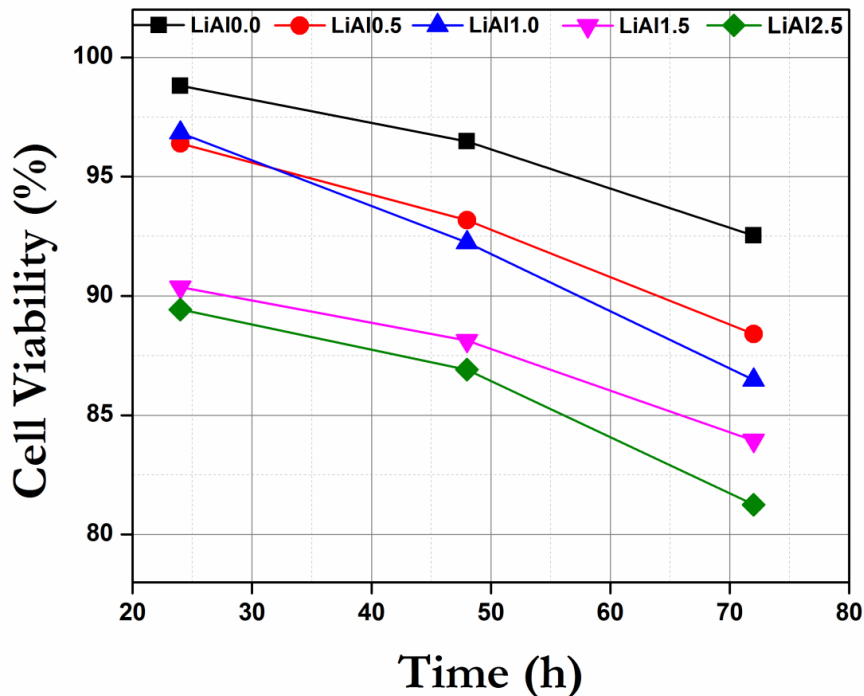

Fig. 3.11: Viability of MG63 cells in the presence of fixed concentration (10 mg/ml) of bioactive glass samples (LiAl0.0 to LiAl2.5).

Moreover, the bioactive glass samples such as LiAl0.0, LiAl0.5 and LiAl1.0 are comparatively less toxic than other glass samples which have been demonstrated by the inhibition of the cell viability in a time dependent manner. The present results suggest that as the concentration of alumina has increased, the cell viability was affected by bioactive glass samples, namely LiAl1.5 and LiAl2.5 (Fig. 3.11). The decrease in cell viability was also supported by growth inhibition of bioactive glass samples when the MG63 cells were cultured in presence of their varying compositions. Similarly, the results on cell cytotoxicity demonstrated the less toxicity against osteoblast MG-63 cell lines as shown in Fig. 3.12.
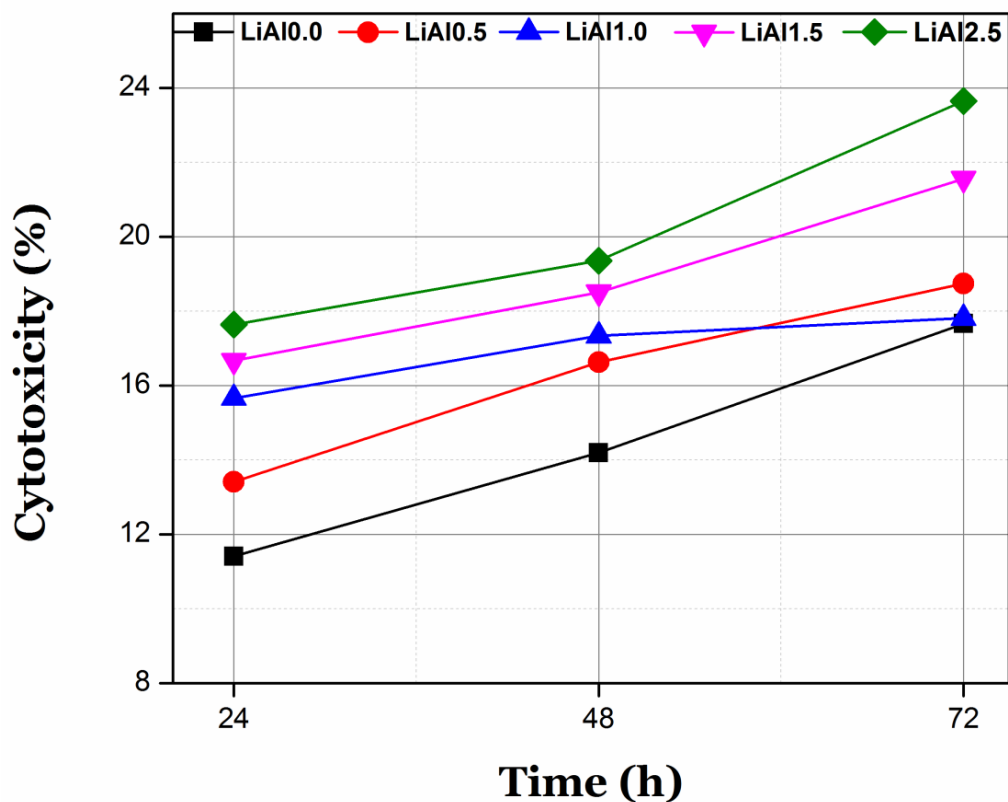

Fig. 3.12: Cytotoxicity of MG63 cells in the presence of fixed concentration (10mg/ml) of bioactive glass samples (LiAl0.0 to LiAl2.5).

The bioactive glass samples; LiAl0.0, LiAl0.5 and LiAl1.0 are also less cytotoxic to MG63 cells as compared to LiAl1.5 and LiAl2.5. The cell viability and cytotoxicity results suggest that bioactive glass samples; LiAl0.0, LiAl0.5 and LiAl1.0 are relatively tolerant to MG63 cell lines in comparison to other samples like LiAl1.5 and LiAl2.5 which causes a decrease in cell viability and direct cellular cytotoxicity.

4. Conclusions

In the present investigation, a comparative study was made on bioactive, physico-chemical and mechanical properties of multi-component Li_2O-CaO-Al_2O_3-P_2O_5-SiO_2 bioactive glasses with varying concentration of Al_2O_3. The following conclusions were drawn from these investigations:

1. On increasing the amount of Al_2O_3 in the bioactive glass samples, density, compressive strength, Vickers hardness and elastic modulus were found to increase accordingly. However, the tendency towards saturation of density beyond 1.0 mol% Al_2O_3 can be due to compensating free volume increase with increasing aluminium leading to asymptotic behavior of change in density in the glass samples.

2. The FTIR absorption spectra showed different characteristic bands because of the silicate network which indicated the formation of hydroxy carbonate apatite (HCA) layer. It is also consistent with the FTIR absorption band at around 546 cm^{-1} due to P-O bending (amorphous) as well as at 960 cm^{-1} attributed due to formation of P-O stretching on the surface of bioactive glass samples after immersing in the SBF solution from 1 to 7 days. The present results regarding formation of HCA in SBF by FTIR absorption spectrometry are well supported by the previous observations.

3. The bioactivity of these samples was measured by *in vitro* test in SBF solution for 1 to 28 days. The pH of the solution was found to increase from 1 to 3 days and then it became nearly constant up to 7 days. After 7 days, the pH of the glass samples decreased which showed a decrease in the bioactivity of the samples. The mechanism of HA formation involved the SiO_2-rich layer formation at the surface of the glass samples which contained Si–OH groups acting as nucleation sites for amorphous calcium–phosphate followed by carbonated hydroxyapatite.

4. The SEM analysis of pre-soaked samples in SBF showed various irregular grains of glass samples. After 28 days of SBF treatment, HCA layer was formed on the surface of these samples due to its bioactive nature. This was also confirmed by X-Ray difractometry of glass samples treated with SBF for 14 days.

5. When alumina was present in small concentrations AlO_6 octahedra dominated the glass structure, whereas AlO_4 tetrahedral units prevailed when Al_2O_3 concentration was higher. Aluminium ions occupy both tetrahedral sites with AlO_4 network former and octahedral with AlO_6 network modifier in the structure. So, the AlO_4 tetrahedra increases the strength of the glass and on the other hand AlO_6 octahedra increases the bioactivity of the bioglass samples.

6. The cell viability and cytotoxicity of bioactive glass samples suggest that these glasses would be useful as bioactive ceramic material which could be achieved by the modifications in molar ratios of Al_2O_3 to make them biocompatible as follows.

7. Finally, we can conclude that the concentration of Al_2O_3 in Li_2O-CaO-Al_2O_3-P_2O_5- SiO_2 glass system should be limited up to 1.5 mol% for a proper balance between

better bioactivity, physico-chemical and mechanical properties for a more suitable bioactive ceramic material.

References:

Abou Neel EA, Pickup DM, Valappil SP, Newport RJ and Knowles JC, Bioactive functional materials: a perspective on phosphate-based glasses, J Mater Chem, 19, 690–701, 2009.

Agathopoulos S, Tulaganov DU, Ventura JMG, Kannan S, Karakassides MA and Ferreira JMF, Formation of hydroxyapatite onto glasses of the $CaO-MgO-SiO_2$ system with B_2O_3, Na_2O, CaF_2 and P_2O_5 additives, Biomaterials, 27, 1832-1840, 2006.

Andersson OH and Sodergard A, Solubility and film formation of phosphate and alumina containing silicate glasses, J, Non- Crys Solids, 246, 9-15,1999.

Arstila H, Hupa L, Karlsson KH and Hupa M, Influence of heat treatment on crystallization of bioactive glasses, J Non-Crystalline Solids, 354, 722–728, 2008.

Belkebir A, Rocha J, Esculcas AP, Berthet P, Gilbert BZ and Gabelica, Structural characterization of glassy phases in the system $Na_2O–Al_2O_3–P_2O_5$ by MAS and solution NMR, EXAFS and vibrational spectroscopy Spectro Acta, 55, 1323–1336, 1999.

Bohner M and Lemaitre J, Can bioactivity be tested in vitro with SBF solution?, Biomaterials, 30, 2175–2179, 2009.

Branda F, Costantini A, Luciani G and Laudisio G, The role of trivalent element oxides in CaO (Na_2O)-M_2O_3-SiO_2 glasses from Tg, J Ther Analy and Calori, 64, 1017-1024, 2001.

Brow RK and Tallant DR, Structural design of sealing glasses, J Non- Crys Solids, 222, 396–406, 1997.

Cao W and Hench LL, Bioactive Materials, Ceramics International, 22, 493–507, 1996.

Cerruti Marta, Greenspan David and Powers Kevin, Effect of pH and ionic strength on the reactivity of Bioglass 45S5, Biomaterials, 26, 1665–1674, 2005.

Clark and L.L. Hench, The influence of surface chemistry on implant interface, J Biomed Mater Res, 10,161-174, 1976.

Clement-Lacroix P, Morvan F, Roman S, Vayssiere B, Belleville C, Lrp5-independent activation of Wnt signaling by lithium chloride increases bone formation and bone mass in mice, Proc Natl Acad Sci, 102, 17406–17411, 2005.

Elliot JC, Structure and chemistry of the apatites and other calcium orthophosphates. Amsterdam, Elsevier Science, 1994.

ElBatal HA, Azooz MA, Khalil EMA, Monem A Soltan, Hamdy YM, Characterization of some bioglass–ceramics, Materials Chemistry and Physics, 80, 599–609, 2003.

El-Kheshen A, Khaliafa FA, Saad EA, Elwan RL, Effect of Al_2O_3 addition on bioactivity, thermal and mechanical properties of some bioactive glasses, Ceramics International, 34, 1667–1673, 2008.

Filgueiras MR, LaTorre G and Hench LL, Solution effects on the surface reactions of three bioactive glass compositions, J Biomed Mater Res, 27 (12), 1485–1493, 1993.

Gisbon IR, Rehman I, Best SM and Bonfield W, Characterization of the transformation from calcium-deficient apatite to b-tricalcium phosphate, J Mater Sci, 12, 799–804, 2000.

Goh Yi-Fan, Alshemary Ammar Z, Akram Muhammad, Kadir Mohammed Rafiq Abdul and Hussain Rafaqat, In-vitro characterization of antibacterial bioactive glass containing ceria, Ceramics International, 40(1 A), 729–737, 2014.

Greenspan D.C. and Hench L.L. Chemical and mechanical behaviour of bioglass coated alumina, J Biomed Mat Res, 10, 503–509, 1976.

Gross U and Strunz V, The interface of various glasses and glass ceramics with a bony implantation bed, J Biomed Mat Res, 19, 251–271, 1985.

Groot K. de, Wolke JGC, Jansen JA, Calcium phosphate coatings for medical implants, Proceedings of the International Mechanical Engineers, 212 Part H, 137–147,1998.

Hanan H Beherei, Khaled R Mohamed and Gehan T El-Bassyouni, Fabrication and characterization of bioactive glass (45S5)/titania biocomposites, Ceramic International, 35, 1991-1997, 2009.

Hayakawa Satoshi, Tsuru Kanji, Ohtsuki Chikara and Osaka Akiyoshi, Mechanism of Apatite Formation on a Sodium Silicate Glass in a Simulated Body Fluid, J Am Ceram Soc, 82, 2155–2160, 1999.

Hench LL, Splinter RJ, Allen WC, Greenlee TK, Bonding mechanisms at the interface of ceramic prosthetic materials, J Biomed Mater Res Symp, 334, 117–141, 1971.

Hench LL, Bioceramics: From concept to clinic, J Am Ceram Soc, 74, 1487- 1510, 1991.

Hench LL, The story of Bioglass, J Mater Sci Mater Med 17, 967-978, 2006.

Jung SB, Day DE, Day T, Stoecker W and Taylor P, Treatment of non-healing diabetic venous stasis ulcers with bioactive glass nanofibers, Wound Repair Regen 30, 19, 2011.

Kasuga Toshihiro, Hosoi Yoshimasa, Nogami Masayuki and Niinomi Mitsuo, Apatite Formation on Calcium Phosphate Invert Glasses in Simulated Body Fluid, J Am Ceram Soc, 84, 45-52, 2001.

Kapusetti G, Misra N, Singh V, Kushwaha R K and Maiti P, Bone cement/layered double hydroxide nanocomposites as potential biomaterials for joint implant, J Biomed Mater Res Part A, 100A, 3363–3373, 2012.

Kapusetti G, Misra N, Singh V, Srivastava S, Roy P, Dana K, Bone cement based nano hybrid as a super biomaterial for bone healing, J Mater Chem B, 2, 3984, 2014.

Kokubo T, Bioactive glass-ceramics properties and applications, Biomaterials, 12, 155–163, 1991.

Kutbay Isil, Yilmaz Bengi, Evis Zafer and Usta Metin, Effect of calcium fluoride on mechanical behavior and sinterability of nano-hydroxyapatite and titania composites, Ceramics International, 40, 14817–14826, 2014.

Kusabiraki Kiyoshi, Infrared spectra of vitreous silica and sodium silicates containing titanium, J Non- Crys Solids, 79 (1–2), 208–212, 1986.

Li P, Zhang F and Kokubo T, The effect of residual glassy phase in a bioactive glass–ceramic on the formation of its surface apatite layer in vitro, J Mat Sci Mat in Medi, 3, 452–456, 1992.

Le Geros RZ, Properties of osteoconductive biomaterials: calcium phosphates. Clin Orthop Relat Res, 395, 81–98, 2002.

Macon Anthony LB, Taek B Kim, Esther M Valliant, Kathryn Goetschius, Richard K Brow, Delbert E Day, Alexander Hoppe, Aldo R Boccaccini, Ill Yong Kim, Chikara Ohtsuki,Tadashi Kokubo, Akiyoshi Osaka, Maria Vallet-Regı´, Daniel Arcos, Leandro Fraile, Antonio J Salinas, Alexandra V Teixeira, Yuliya Vueva, Rui M Almeida, Marta Miola, Chiara Vitale-Brovarone, Enrica Verne, Wolfram Holand and Julian R. Jones, A unified in vitro evaluation for apatite-forming ability of bioactive glasses and their variants, J Mater Sci Mater Med, 26, 115, 2015.

Majhi MR, Pyare R and Singh SP, Preparation and characterization of CaF_2 doped bioglass ceramics, J Biomim Biomat & Tissue Eng, 11, 45-66, 2011.

Majhi MR, Kumar R, Singh SP and Pyare R, Physico-chemical properties and characterization of CaO-Fe$_2$O$_3$-P$_2$O$_5$ glass as a bioactive ceramic material. J Biomim Biomat & Tissue Eng, 12, 1-24, 2012.

Majhi MR, Pyare R and Singh SP, Studies on preparation and characterizations of CaO-Na2O-SiO2-P2O5 bioglass ceramics substituted with Al$_2$O$_3$, TiO$_2$ and ZrO$_2$, J Biomim Biomat & Tissue Eng, 2, 1-17, 2012.

Marti, Dr. Robert Mathys Foundation, Bischmattstr. 12, CH-2544 Bettlach, Inert bioceramics (Al$_2$O$_3$, ZrO$_2$) for medical application, Injury-international Journal of The Care of The INJURY-INT J CARE INJURED 01/2000; 31. DOI:10.1016/S0020-1383(00)80021-2.

Mirhadia B and Mehdikhanib B, Investigation of crystallization and microstructure of Na$_2$O-CaO-P$_2$O$_5$-SiO$_2$-Al$_2$O$_3$ bio glass ceramic system, N J Glass & Cera, 2, 1-6, 2012.

Mohini GJ, Krishnamacharyulu N, Baskaran GS, Rao PV and Veeraiah N, Studies on influence of aluminium ions on the bioactivity of B$_2$O$_3$–SiO$_2$–P$_2$O$_5$–Na$_2$O–CaO glass system by means of spectroscopic studies, App Sur Sci, 287, 46-53, 2013.

Muller D, Berger G, Grunze I, Ludwig G, Hallas E and Haubenreisser U, Solid state high-resolution 27A1 nuclear magnetic resonance studies of the structure of CaO-Al$_2$O$_3$-P$_2$O$_5$ glasses, Phys Chem Glasses, 24, 37–42, 1983.

Nakamura M, Mochizuki Y, Usami K, Itoh Y and Nozaki T, Infrared absorption spectra and compositions of evaporated silicon oxides (SiOx), Sol Sta Commn, 50, 1079–1081, 1984.

Ohtsuki C, Kokubo T and Yamamuro T, Compositional dependence of bioactivity of glasses in the system CaO–SiO₂–Al₂O₃: it's in vitro evaluation, J Mat Sci Mat in Med, 3, 119–125, 1992.

Paul A and Zaman MS, The relative influences of Al₂O₃ and Fe₂O₃ on the chemical durability of silicate glasses at different pH values, Journal of Materials Science, 13(7), 1499-1502, 1978.

Paul A, Chemistry of glasses, Second Edition, Chapman & Hall, London, 149-151, 1990.

Rahaman MN, Day DE, Bal BS, Q Fu, Jung SB and Bonewald LF, Bioactive glass in tissue engineering, Acta Biomater, 7, 23, 55–2373, 2011.

Scholes SR, Modern glass practice 7th edition, 375, 1975.

Shannon RD, Revised Effective Ionic Radii and Systematic Studies of Interatomic Distances in Halides and Chalcogenides, Acta Cryst Sec A, 32(5), 751–767, 1976.

Shirtliff VJ and Hench LL, Bioactive materials for tissue engineering, regeneration and repair, J Mat Sci, 38, 4697–4707, 2003.

Sitarz M, Bulat K and Szumera M, Aluminium influence on the crystallization and bioactivity of silico-phosphate glasses from NaCaPO₄–SiO₂ system, J Non-Crystalline Solids, 356, 224–231, 2010.

Sitarz M, Structure and texture of glasses belonging to KCaPO₄–SiO₂ and KCaPO₄–SiO₂–AlPO₄ systems, Physics and Chemistry of Glasses, Euro J Glass Sci & Tech, 51, 179–186, 2010.

Stoch A, Jastrzebski W, Brozek A, Trybalska B, Cichocinska M and Szarawara E, FTIR monitoring of the growth of the carbonate containing apatite layers from simulated and natural body fluids, Journal of Molecular Structure, 511–512, 287–294, 1999.

Teixeira Zaine, Oswaldo Luiz Alves and Italo Odone Mazali, Structure, Thermal Behavior, Chemical Durability, and Optical Properties of the $Na_2O–Al_2O_3–TiO_2–Nb_2O_5–P_2O_5$ Glass System, Journal of the American Ceramic Society, 90(1), 256–263, 2007.

Vallet-Reg M, Roma J, Padilla S, Doadrio JC and Gil FJ, Bioactivity and mechanical properties of SiO_2-CaO-P_2O_5 glass ceramics, J Mater Chem 15, 1353–1359, 2005.

Varshneya A K, Fundamentals of Inorganic glasses, 2nd edition, Society of Glass Technology, Sheffield, U.K. pp.129, 515-17, 2006.

Zamani A, Omrani RG and Masoud Mousavi Nasab, Lithium's effect on bone mineral density, Bone, 44, 331–334, 2009.